



HAL
open science

Chemical surface modification of lithium disilicate needles of a silica-based ceramic after HF-etching and ultrasonic bath cleaning: Impact on the chemical bonding with silane

Angeline Poulon-Quintin, Emma Ogden, Axel Large, Mélanie Vaudescal, Christine Labrugère, Michel Bartala, Caroline Bertrand

► To cite this version:

Angeline Poulon-Quintin, Emma Ogden, Axel Large, Mélanie Vaudescal, Christine Labrugère, et al.. Chemical surface modification of lithium disilicate needles of a silica-based ceramic after HF-etching and ultrasonic bath cleaning: Impact on the chemical bonding with silane. *Dental Materials*, 2021, 37 (5), pp.832-839. 10.1016/j.dental.2021.02.006 . hal-03211119

HAL Id: hal-03211119

<https://hal.science/hal-03211119>

Submitted on 28 Apr 2021

HAL is a multi-disciplinary open access archive for the deposit and dissemination of scientific research documents, whether they are published or not. The documents may come from teaching and research institutions in France or abroad, or from public or private research centers.

L'archive ouverte pluridisciplinaire **HAL**, est destinée au dépôt et à la diffusion de documents scientifiques de niveau recherche, publiés ou non, émanant des établissements d'enseignement et de recherche français ou étrangers, des laboratoires publics ou privés.

Chemical surface modification of lithium disilicate needles of a silica-based ceramic after HF-etching and ultrasonic bath cleaning: Impact on the chemical bonding with silane

A. Poulon-Quintin^{a,*}, E. Ogden^a, A. Large^{a,b}, M. Vaudescal^c, C. Labrugère^c, M. Bartala^b, C. Bertrand^{a,b}

^a CNRS, Université de Bordeaux, ICMCB, 87 Avenue du Dr. A. Schweitzer, F-33608, Pessac, France

^b Université de Bordeaux, UFR d'Odontologie, 146 Rue Léo Sagnat, F-33076, Bordeaux, France

^c Université de Bordeaux, PLACAMAT, 87 Avenue du Dr. A. Schweitzer, F-33608, Pessac, France

A B S T R A C T

Keywords:

Lithium disilicate glass-ceramic

HF-etching

Silane

Bonding

Microstructure

Objective. Recommendations to obtain the best bonding to silica-based ceramics are to prepare its surface by hydrofluoric-acid HF etching and regular application of a silane. This study investigated how the HF-etching following by ultrasonic water bath cleaning (recommended protocol to improve the bonding with a composite resin), modifies the surface chemistry of a lithium disilicate glass-ceramic and impacts the chemical bonding with silane.

Methods. Lithium disilicate glass-ceramic discs (IPS Emax Press, Ivoclar Vivadent) were mirror polished, etched with 9% HF for 20 s and rinsed 1 min under water. Two post-etching cleaning were compared: (1) no additional cleaning and (2) immersion in water ultrasonic bath for 4 min. Morphology evolution of the surfaces was carried out by scanning electron microscopy. Chemical changes were studied using X-ray Photoelectron Spectroscopy and Nano Auger Electron Spectroscopy analyses. Identification of the compounds formed with fluorine was based on by High Resolution Transmission Electronic Microscopy .

Results. Residues left on the surface of the discs after etching, the fluorine salts, were eliminated after the ultrasonic bath cleaning. However, analyses showed presence of fluorine on the lithium disilicate needles associated among others with the lithium. HR-TEM validates the presence of Li_2SiF_6 crystallized phased. A mechanism to explain silane bonding when Li_2SiF_6 phase is formed on the $\text{Li}_2\text{Si}_2\text{O}_5$ needles, is proposed.

Significance. HF-etching leads to the formation of lithium and fluorine contain LiSi_2F_6 nano-precipitates on the $\text{Li}_2\text{Si}_2\text{O}_5$ needles which helps to improve the bonding with silane.

* Corresponding author at: ICMCB, 87 Avenue du Dr. A. Schweitzer, F-33608, Pessac, France.

E-mail address: angelina.poulon@icmcb.cnrs.fr (A. Poulon-Quintin).

<https://doi.org/10.1016/j.dental.2021.02.006>

1. Introduction

In recent years, an increasing demand for high performance aesthetic restorations has led to the development of several new ceramics. Heat-pressed or computer-aided design and computer-aided manufacturing (CAD/CAM) fabricated lithium disilicate glass ceramics are preferred over other types of dental ceramics because of these superior characteristics: excellent mechanical properties, accuracy of fit and optical properties that mimic those of natural teeth [1]. In dentistry, each restoration has two interfaces: tooth/resin and resin/ceramic. In this study, we will focus on the resin/ceramic interface known to be in general weaker than the tooth/resin one. There are many reasons for the dental ceramics to fracture, e.g. mastication, parafunction and intraoral occlusal forces creating repetitive dynamic loading. Thus, the establishment of a durable and reliable bond between a dental ceramic and a resin composite is important in dental practice. This bond is usually created via two mechanisms, micro-mechanical attachment thanks to HF-etching and chemical bonding thanks to the silane molecules. Silanes are silicon esters that may contain trialkoxysilane groups. There are hybrid functional monomers capable of forming chemical bonds with organic and inorganic surfaces. In general, silanes have non-hydrolysable groups (such as methacrylate) and hydrolysable groups (such as ethoxy), which is why they are chemically bifunctional. They bond dissimilar materials together by forming a branched 3D siloxane ($-\text{Si}-\text{O}-\text{Si}-$) film. In addition to their chemical bonding power, silanes are used as surface primer agents for adhesion promotion that can increase the critical surface energy of a substrate. A high critical surface energy and a low surface tension of a liquid are desired because liquids will spread evenly onto the surface. In order to achieve complete wetting, the adhesive must have low viscosity and the surface tension must be lower than the critical surface tension (γ_c) of the substrate surface [2]. An optimal silane application implies the elimination of water, alcohol and other solvents, allowing for the complete condensation reaction to form the siloxane bond and eliminate excess silane oligomers to obtain a monolayer silane [3,4]. The stability and effectiveness of this adhesion is also supposed to be improved by heat treatment [5–9] but Bruzi et al. study based on the evaluation of the shear bond strength of composite resin to CAD/CAM lithium disilicate ceramics after different post-etching cleaning and silane treatments, recommends a regular application of silane (applied for 20 s, air dried for 20 s and hot dried at 60 °C for 20 s).

The silane most used in dentistry is the MPS (γ -methacryloxypropyl trimethoxysilane or $\text{C}_{10}\text{H}_{20}\text{O}_5\text{Si}$) coupling molecule (geometry shown in Fig. 1).

The HF-etching is known to provide the dissolution of the glassy and/or crystalline phase [11] and to leave residual salts of silicafluoride negatively influencing the resin bond strength [12,13]. Several cleaning methods are suggested in literature but the most supported post-etching protocol is the use of ultrasonic distilled water bath for 2 min [10,12,14,15].

This study proposes to investigate how the HF-etching following by ultrasonic water bath cleaning (recommended protocol to improve the bonding with a composite resin), mod-

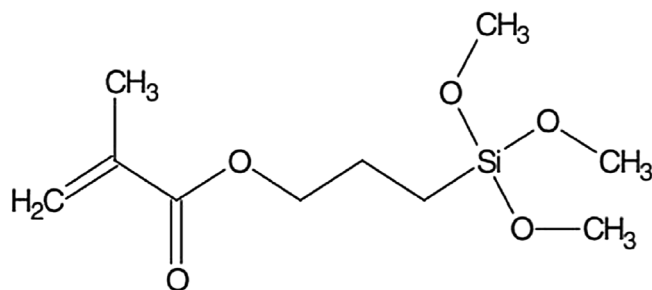


Fig. 1 – Representation of the MPS (γ -methacryloxypropyl trimethoxysilane or $\text{C}_{10}\text{H}_{20}\text{O}_5\text{Si}$) in 2D.

ifies the surface chemistry of a lithium disilicate glass-ceramic with only a focus on the $\text{Li}_2\text{Si}_2\text{O}_5$ crystal surfaces, and impacts the chemical bonding with silane.

2. Materials and methods

The lithium disilicate glass-ceramic (IPS Emax Press, Ivoclar Vivadent) tested samples were in the form of pellets (diameter: 1.9 cm; thickness: 4 mm) with parallel faces. The global composition announced by the Ivoclar/Vivadent supplier is (in wt%): SiO_2 57–80, Li_2O 11–19, K_2O 0–13, P_2O_5 0–11, ZrO_2 0–8, ZnO 0–8 and other oxides as Al_2O_3 0–10. One face of each sample was first mirror-polished.

This face was before HF-etched applying 9% hydrofluoric acid (Porcelain Etch[®], Ultradent) for 20 s (recommended action time by Ivoclar-Vivadent) and then rinsed 1 min with water as dentists done. To rinse, no distilled water was used like it can be read in the literature. In the dentist protocol, there is also no control of the amount of HF deposited, the only criterion retained by the practitioner being a covering of the entire surface of the ceramic by the HF acid. To improve the reproducibility of our results, the quantities of acid deposited were weighed. For each sample, the same quantities of HF were applied (25 mg) by a professional dentist with the same gesture as in its dental office for preparation of the restoration surfaces. Other samples were etched and rinsed as the previous ones but also immersed in water ultrasonic bath (WUS bath) for 4 min.

Only the central parts of the samples were studied.

To evaluate the crystallized phases present, XRD analysis was performed with a PANalytical X'Pert Pro device ($\lambda(\text{CuK}\alpha) = 1.5418 \text{ \AA}$, $2\theta = 10\text{--}80^\circ$, step of $0,01^\circ$).

SEM images (conventional JSM6360A JEOL, 10 kV, sample beforehand metalized with thin gold layer) were used to follow the evolution of the morphology of the surface.

X-ray Photoelectron Spectroscopy XPS surface analysis were performed using a Thermo-Fisher Scientific K-ALPHA spectrometer with a monochromatized $\text{AlK}\alpha$ source ($h\nu = 1486.6 \text{ eV}$) and a $200 \mu\text{m}$ X-Ray spot size. A pressure of 10^{-7} Pa was reached in the chamber when transferring the HF-etched samples. The full spectra (0–2100 eV) were obtained with a constant pass energy of 200 eV and high resolution spectra (i.e. C1s, O1s, F1s, Li1s, K1s, Si2p, Au3d) at a constant pass energy of 40 eV. Charge neutralization was applied during analysis and sputtering was achieved through low energy Ar^+ ions.

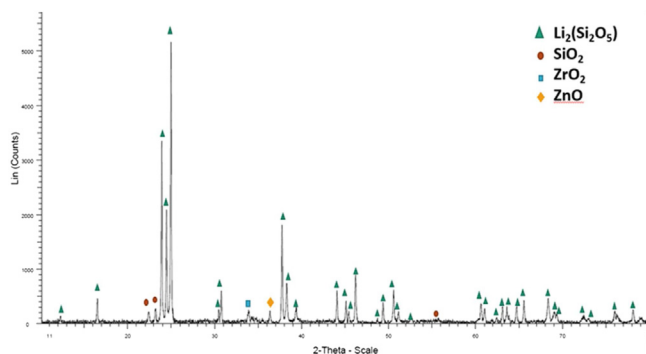


Fig. 2 – XRD pattern obtained on a lithium disilicate glass-ceramic pellet (IPS Emax Press, Ivoclar Vivadent). 4 crystallized phases: $\text{Li}_2\text{Si}_2\text{O}_5$ (ICDD card 01-070-4856), ZrO_2 (ICDD card 01-079-1796), ZnO (ICDD card 00-036-1451) and SiO_2 (ICDD card 00-051-1379).

The PHI 710 Auger nanoprobe spectroscope used was equipped with an Argon ion gun and a cylindrical mirror analyser (CMA) with energy resolution varying from 0.1 to 0.5 % with also the advantage of excellent spatial in width and depth resolution resp. (10 nm and 5 nm). The AES analyses were semi-quantitative and particularly sensitive for light elements. Line analyses were performed (10 kV electron beam voltage and 2 nA for current). Prior to Auger analysis, argon sputtering was done at 2 kV, during 60 s with an ion current of 3 μA to remove the carbon contamination and most of the gold metallization. Each elemental line trace consists of 512 data points with their intensity corresponding to the peak-to-peak intensity of the element's derivative Auger spectrum (dN/dE versus kinetic energy).

For TEM analyses, thin foils were prepared at the liquid nitrogen temperature using an EM-09100 cryo-ion slicer system (JEOL, Tokyo, Japan). The treated-surfaces were previously coated with gold to clearly visualised the top free surfaces and also avoid charging problem during observations. They were then prepared to observed in cross-section the different interfaces. Observations were carried out on a JEOL 2200FX (JEOL, Tokyo, Japan) operated at 200 kV.

3. Results

3.1. The lithium disilicate glass-ceramic

The XRD pattern of one lithium disilicate glass-ceramic pellet (Fig. 2) allows to identify four crystallized phases: lithium disilicate ($\text{Li}_2\text{Si}_2\text{O}_5$, ICDD card 01-070-4856), zirconium oxide (ZrO_2 , ICDD card 01-079-1796), zinc oxide (ZnO , ICDD card 00-036-1451) and cristobalite (SiO_2 , ICDD card 00-051-1379). The other components no detected by XDR could be glassed, imperfectly crystallized, nanosized or in too small quantities to be detected.

3.2. Evolution of the surface morphology after HF etching

Fig. 3 shows the morphology evolution of the IPS Emax Press lithium disilicate glass-ceramic pellet thanks to SEM images.

Fig. 3a is an image of the mirror polish surface realized in chemical contrast (BSE-SEM). Presence of a darker phase with elongated form and surrounding by a whiter one identified as the glassy phase can be notice. This result is in agreement with the morphology after HF-etching presented on Fig. 3c. Fig. 3b is a SEM image of the $\text{Li}_2\text{Si}_2\text{O}_5$ crystals from Ivoclar Vivadent after HF vapour etching for 30 s of the IPS Emax Press lithium disilicate glass-ceramic. Comparison of this image with the morphology obtained after aqueous HF etching (20 s) following by 1 min water rinsing (Fig. 3c), two major differences appear: (1) the crystals are not clearly observable due to the presence of residues (residual glassy phase and residual salts of silicafluoride) and (2) The crystals seems to be thinner and shorter. When an additional cleaning step using WUS for 4 min is added (Fig. 3d), no more residue is observable on the surface and the reduction of the $\text{Li}_2\text{Si}_2\text{O}_5$ crystals dimensions is confirmed.

3.3. Study of the fluorine presence after WUS cleaning

HF-etching is known to leave residual salts of silica fluoride that precipitate and can be identified as a white deposit on the etched ceramic surface [16]. During WUS, the formation of microscopic bubbles causes the detachment of impurities even in inaccessible recesses. This gentle cleaning method eliminates all residues, dirt, oxidation products, deposits etc. and contaminants from all surfaces [17,18]. TEM observations show that there is a thickness reduction of the HF-affected “layer” (around few μm for HF-etched water rinsed 20 s sample and difficult to defined when WUS cleaned) and confirms the departure of the salts but also the removing of the no-well entrapped phases in the glassy materials as $\text{Li}_2\text{Si}_2\text{O}_5$ crystals (Fig. 4).

F1s XPS spectra are presented Fig. 5 to validate the efficiency of the WUS cleaning and the departure of the residual salts of silica fluoride or other compounds containing fluorine. The binding energy of fluorine F1s is known to be around 686–689 eV. Comparing the curve (Fig. 5a) of the HF-etched water rinsed sample (in red) with the HF-etched, water rinsed sample and WUS cleaned sample (in dark blue), a significant reduction of the F1s peak is observable. This last sample is etched again during 60 s with argon ions inside the XPS chamber after the first previous analyse. The F1s spectrum is acquired again for the same area (in light blue). The disappearance of a small F1s peak is observable. Same protocol of argon etching is used on the HF-etched water rinsed sample for 60, 120 and 600 s of cumulative argon etching time (Fig. 5b). There is no significant change of the F1s peak. These results are in agreement with the TEM observations: the thickness affected by the HF-etched and water rinsed sample is higher than with the use of an additional WUS cleaning where only the extreme top surface seems to be affected.

3.4. Localisation of the fluorine presence after WUS cleaning

Because the XPS analysed surface is around 200 μm in diameter and due to the roughness of the samples after WUS cleaning (Fig. 3d), AES line analyses along lithium disilicate elongated crystals are realized. An example of results obtained

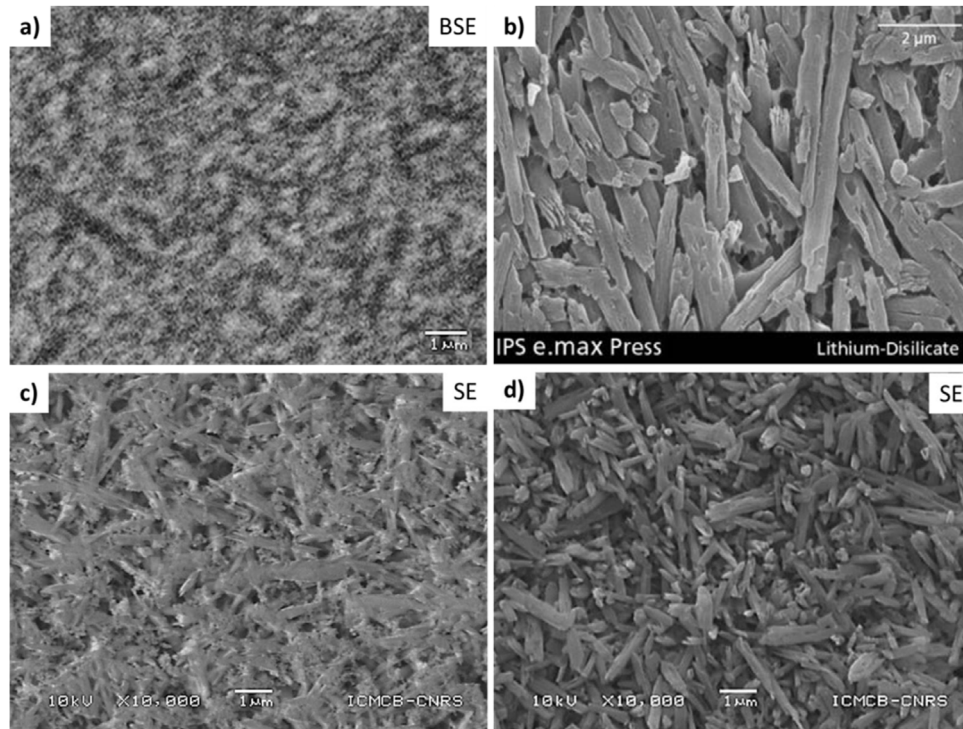


Fig. 3 – Microstructure of IPS e.max Press lithium disilicate glass-ceramic: (a) mirror polished, (b) etched with HF vapour for 30 s (image from Ivoclar Vivadent), (c) HF-etched 20 s and water rinsed 1 min and (d) HF-etched 20 s, water rinsed 1 min and WUS cleaned 4 min.

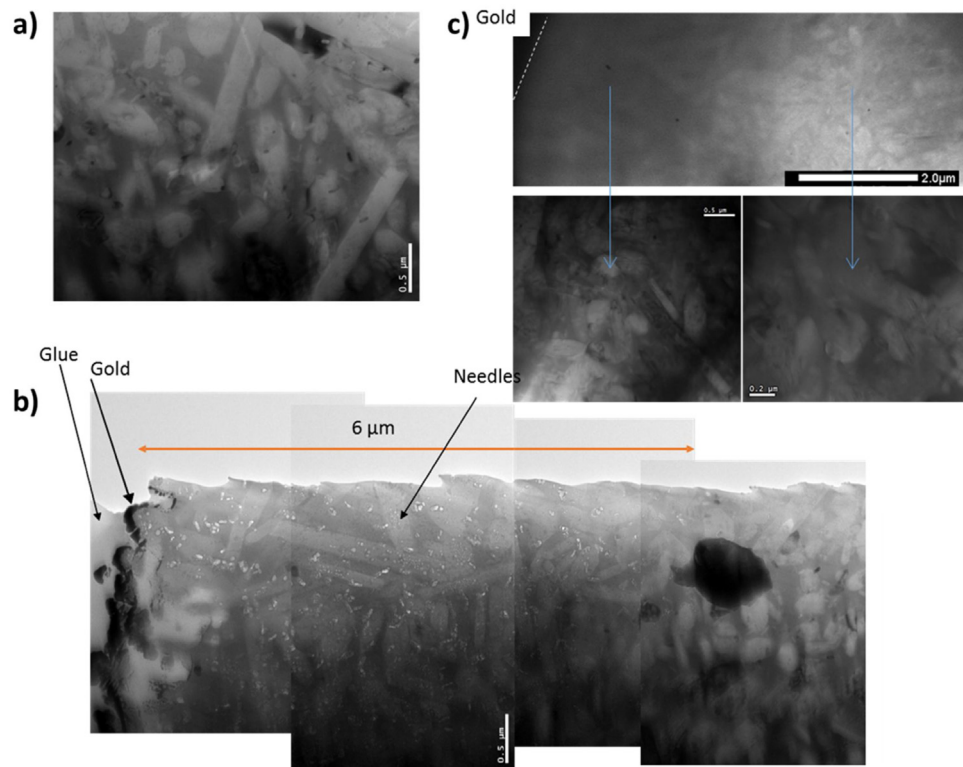


Fig. 4 – Bright-Field-TEM images of samples (a) as received, (b) HF-etched water rinsed 20 s and (c) WUS cleaned 4 min.

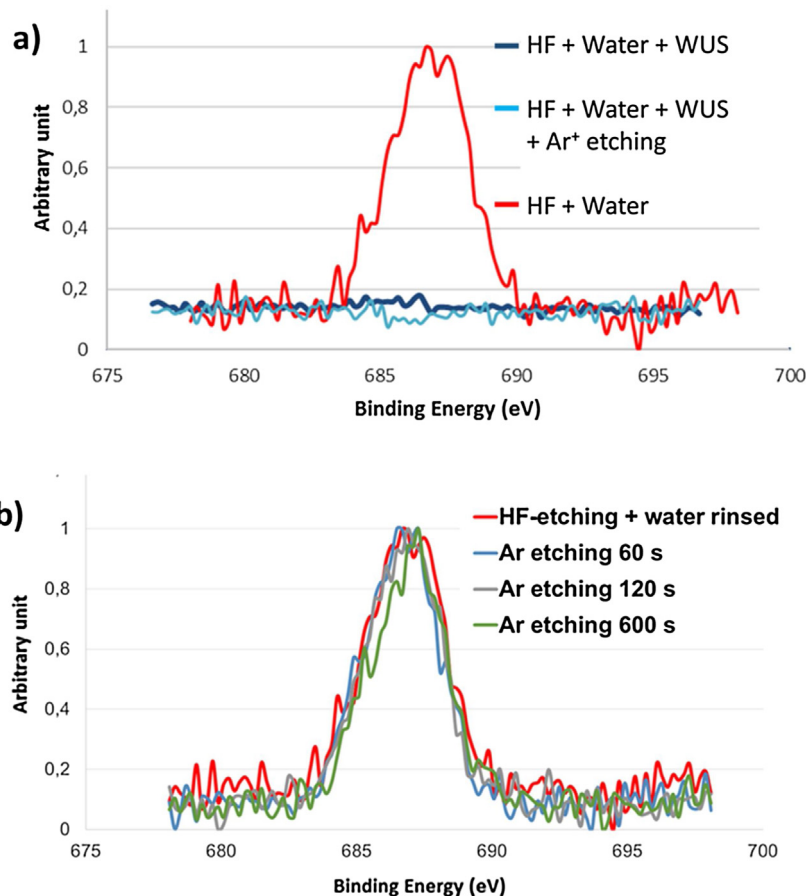


Fig. 5 – (a) Overlapping graph of XPS F1s curves on 2 samples: (1) HF-etched 20 s and then rinsed with water 1 min (in red), 2) WUS rinsed 4 min (dark blue) and then additionally argon etched 60 s (light blue). (b) XPS F1s curves of the HF-etched 20 s and then rinsed with water 1 min (in red) and then additionally argon etched 60, 120 and 600 s (additional argon etchings on the same area; cumulative time) (For interpretation of the references to colour in the figure legend and text, the reader is referred to the web version of this article.).

is presented Fig. 6. In extreme surface, when fluorine appears, lithium and oxygen are always combined with. The length affected by fluorine is around 100 nm. Even after WUS cleaning, fluorine is still present at the extreme surface of the needles. Quantification in atomic percent of fluorine, lithium and potassium realized on another crystal helps to conclude that the ratio between F and Li varies from 4 to 7 and that sometimes fluorine is not combined with Li or K. When F is present with K, the ratio between K and F is around 3.

4. Discussion

The evolution of the lithium disilicate glass-ceramic disc surface after HF-etching is conventional with the dissolution of the glassy phase following the identified well known scenario. The acid reacts with the silica matrix to form volatile silicon tetrafluoride SiF_4 and creates a porous structure [19,20].

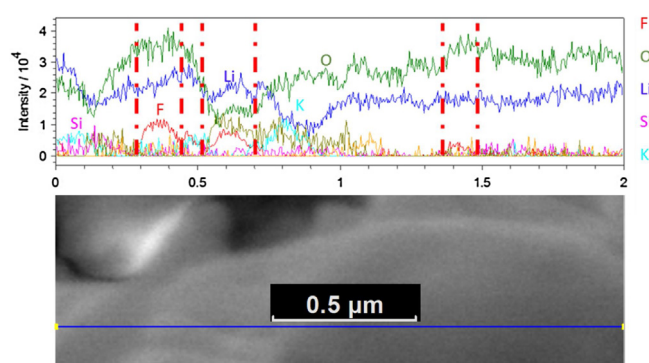
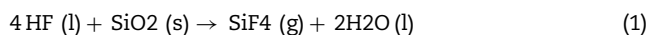
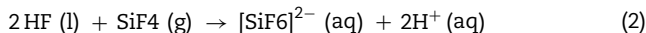
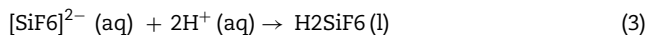


Fig. 6 – Secondary electron micrograph of the needle with the position of the horizontal line analysed (in blue) and the corresponding elemental line AES analysis (in intensity) for a HF-etched 20 s, water rinsed 1 min and WUS4 min cleaned sample. (For interpretation of the references to colour in the figure legend, the reader is referred to the web version of this article.)

Then, SiF₄ reacts further with the hydrofluoric acid again to form a soluble complex ion, hexafluorosilicate [SiF₆]²⁻ and hydrogen ions.



The hydrogen ions in the solution react with the hexafluorosilicate complex ion to form a fluorosilicic acid that can be rinsed off:



Depending on the practitioner techniques, the quantity and the concentration used as the duration of etching performed, the glassy matrix is more or less dissolved. Etching alters surface topography by creating micro- and nano-scale porosities of varying depth and width [21]. This porous surface is not only providing more surface area for resin bonding, but also exposes and generates hydroxyl groups on the ceramic surface that are responsible for chemical bonding via silane coupling agents.

However, the HF-etching is also known to react with crystallised phases [11,21]. The glassy phase dissolves at a faster rate than the crystallized phases but no more information is given about presence of fluorine on the lithium disilicate crystal in literature to our knowledge. Figs. 3c and 4 are in agreement with the results found in literature with an affected depth around 6 μm (small pores observables on Fig. 4) and a modification of the surface morphology with the presence of pores. On TEM images, Li₂Si₂O₅ crystals look like pillars of needles randomly oriented and entrapped in the glassy matrix.

An additional WUS cleaning leads to the departure of the fluorine salts as already observed by other authors [12,13,20,21]. The efficiency of the distilled water ultrasonic bath is clearly identified in the literature as the best post-etching cleaning to positively improves the resin shear bond strength [10,17,18]. In this study, a conventional process of HF-etching is used whereas the supplier etches with HF vapour for 30 s (Fig. 3b, image from Ivoclar Vivadent). Pillars of plate-like Li₂Si₂O₅ crystals and no glassy phase are observable.

After WUS cleaning, all the fluorine salts, residues and no adherent phases are removed from the surface as XPS analyses confirm (Fig. 5a) whereas they are still present at a greater depth when only water rinsing is used (Fig. 5b).

Another key point is the Li₂Si₂O₅ crystals morphology changes. They seem to be no more plate-like but more sharpen (Fig. 3d) and rounder (Figs. 6 and 7) so named needles. AES local analyses in line on the extreme surface of these needles confirm a localised presence of fluorine on their surface (about 100 nm long) and most of the time combined with lithium and oxygen. Bischoff et al. [22] working on lithium disilicate glass-ceramics based on non-stoichiometric compositions, conclude to the absence of lithium ion clustering in the glassy component of the final glass-ceramic and also argue against an epitaxial nucleation process proposed in literature. They suggest the nucleation of Li₂Si₂O₅ starts at the disordered lithium phosphate phase (Li₃PO₄) and the glassy matrix. But in the lithium silicate glass system, Puls and Eckert give clear evidence of strong lithium cation clustering providing quantitative support for a model of one dimensional chan-

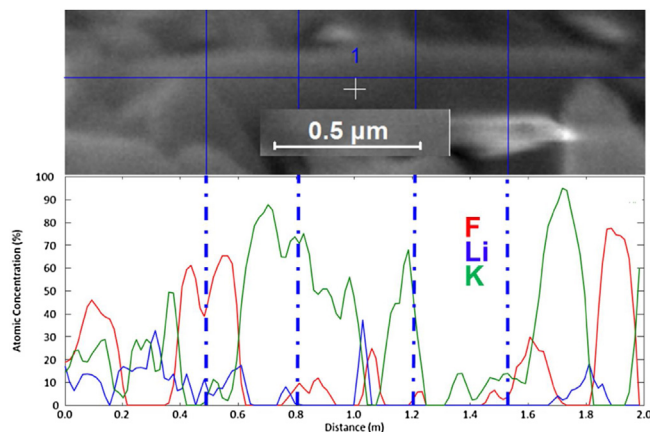


Fig. 7 – Secondary electron micrograph of a needle with the position of the horizontal line analysed (in blue) and quantitative AES analysis of F, Li and K for a HF-etched 20 s, water rinsed 1 min and WUS 4 min cleaned sample. (For interpretation of the references to colour in the figure legend, the reader is referred to the web version of this article.)

nel structure in (Li₂O)_x(SiO₂)_{1-x} with $x \leq 0.3$ [23]. This study indicates that the structure of low lithium silicate glasses is consistent with the formation of lithium rich quasi-one-dimensional channels, in which each Q⁽³⁾-silicon species is surrounded by about three lithium ions. Each lithium atom is surrounded by three non-bridging oxygen atoms. The structure of Li₂Si₂O₅, layered plate-like crystals is similar to the previously described for the glassy phase. They are composed of [SiO₄] tetrahedra sharing corners, Li atoms with presence of channels [24]. A representation of the needle free surface and of the Li₂Si₂O₅ layered structure of crystal phase is proposed by Upadhyaya et al. [25] without taking into account the presence of fluorine. In these crystals, Q⁽²⁾ and Q⁽⁴⁾-silicon structure of [SiO₄] tetrahedra are also present [26].

In this study, XPS analyses not allow to find information about the types of fluorine chemical bonding and AES about the global composition due the technique protocol itself and also to charging phenomenon for long duration. To try to identify if the fluorine is combined with others elements to create a crystallised compound on the Li₂Si₂O₅ needle surface, HRTEM study of the extreme surface of needles localised at the free surface of the WUS cleaned samples is carried out.

Fig. 8a is a bright-field TEM image (BF-TEM) of the free sample surface after HF-etching, water rinsing and WUS cleaning. The compound in extreme surface of the needles is oriented to be in Bragg position to reveal the presence of small plate-like particles of about 100 nm length (observable in dark inside red circles, Fig. 8a). Their longer face is always parallel to the free surface of the needles. Their dimensions are coherent with AES results. HRTEM analyses are carried out in order to identify the compound formed based on the previous chemical information collected. These small plate-like particles are identified as SiLi₂F₆ phase. This result is illustrated on Fig. 8b (original HR-TEM image on left and overlapping of the colorized corresponding inverse FFT images on right). The area of interest is between the two previous images.

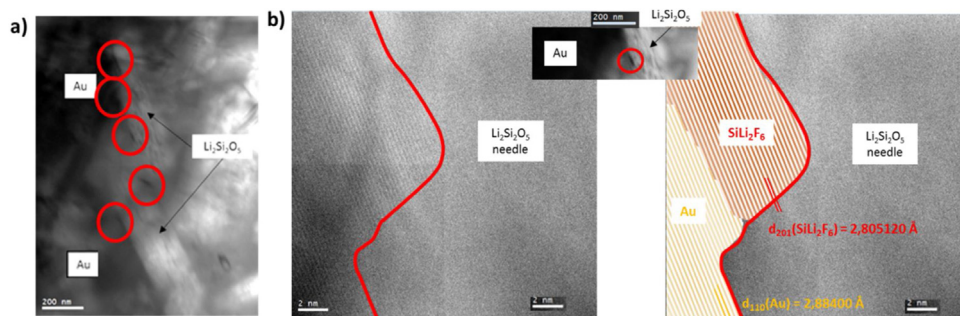


Fig. 8 – (a) BF-TEM image of the free surface for a HF-etched and WUS cleaned sample, (b) HRTEM images of the interface between a $\text{Li}_2\text{Si}_2\text{O}_5$ crystallised needle and a small plate-like particle identified as SiLi_2F_6 (Au used as conductive coating). (For interpretation of the references to colour in the text, the reader is referred to the web version of this article.)

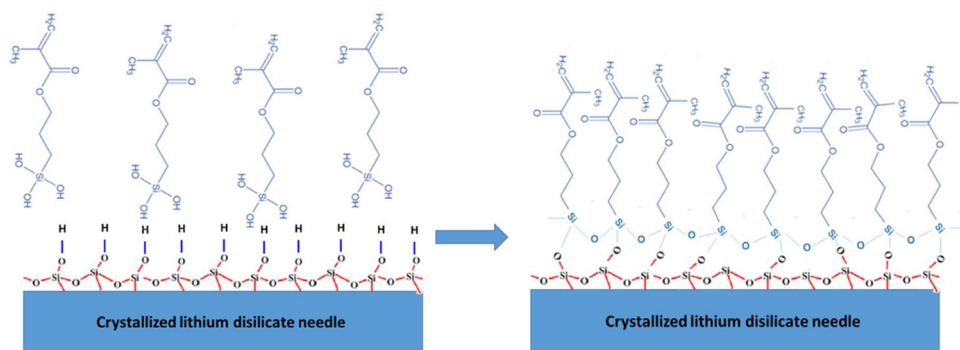
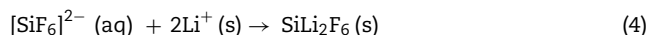
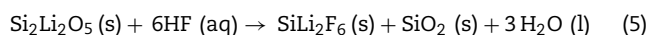


Fig. 9 – Idealized illustration of how silane compounds chemically bond to inorganic silica when SiLi_2F_6 small plate-like particles are present on the crystallized $\text{Li}_2\text{Si}_2\text{O}_5$ needles surface and leads to the densification of the 3D siloxane network at the surface of the needles.

Fig. 9 proposed an idealized mechanism based on the mechanism proposed by Shrivastava [27] to explain silane bonding when crystallized SiLi_2F_6 small plate-like particles are present on the $\text{Li}_2\text{Si}_2\text{O}_5$ needles surface. As for the glassy phase, HF-etching of the needles leads to the formation of hexafluorosilicate $\text{SiF}_6^{2-}(\text{aq})$. The VSEPR predicts for $[\text{SiF}_6]^{2-}$ the octahedral shape. Thanks to the removing of silica, hexafluorosilicate complex ions can react with the lithium ions to form a SiLi_2F_6 solid at the needle surface:



A global reaction between lithium disilicate needles and hydrofluoric acid leading to the formation of silica and water is proposed:



Additional HRTEM observations have to be done to find if orientation relationships exist between the two phases. However, the local modification of the needle roughness is observable due to the formation of the SiLi_2F_6 plate-like particles.

When the silane is applied over the etched ceramic surface, the molecule is activated by hydrolysis to form silanol groups ($-\text{Si}-\text{O}-\text{Si}-$) which react with the substrate surface hydroxyl ($-\text{OH}$) groups by a condensation reaction. There is the formation of a branched 3D siloxane ($-\text{Si}-\text{O}-\text{Si}-$) film [28].

As a consequence of the previous chemical reaction, some $-\text{Si}-\text{O}-\text{Si}-$ assemblies are broken on the $\text{Li}_2\text{Si}_2\text{O}_5$ needles surface which could facilitate the formation of hydroxyl species around these small plate-like particles. For a same quantity of HF used for etching, an increase of the number of bonds with $-\text{OH}$ compare to the number formed on a same needle surface for a water rinsed sample could explain the improvement of the WUS sample bonding properties (to be published) for two reasons: (1) the direct access to the surface of the interlocked needles thanks to the departure of all the salts, residues, etc. and (2) the densification of the 3D siloxane network close to the surface of the needles due to the increase of the hydroxyl groups in surface. The role of the SiLi_2F_6 small plate-like particles seems also to be the increase of the needle surface nano-roughness. At the moment no evidence of their bonding with silane compound is proved.

Fig. 9 proposed an idealised illustration of how silane compounds chemically bond to inorganic silica when SiLi_2F_6 small plate-like particles are present on the crystallized $\text{Li}_2\text{Si}_2\text{O}_5$ needles surface after the hydrolysis reaction of γ -methacryloxypropyltrimethoxysilane to form silanol groups ($-\text{Si}-\text{O}-\text{Si}-$).

5. Conclusion

In the literature, the protocol to obtain the best bonding to lithium disilicate glass-ceramics is to prepare its surface

by hydrofluoric-acid HF etching 20 s, water rinsing 1 min and then immersion in water ultrasonic bath for 4 min. A regular application of a silane compound MPS in this study (γ -methacryloxypropyl trimethoxysilane or $C_{10}H_{20}O_5Si$) applied for 20 s, air dried for 20 s and hot dried at 60 °C for 20 s is required before the application of the resin.

Thanks to the fine analyze of the $Li_2Si_2O_5$ crystals free surface after the HF-etching, the presence of crystalized small plate-like particles identified as $SiLi_2F_6$ is proved. Due to their presence, the improvement of the bonding is explained by the creation of additional nano-roughness on the $Li_2Si_2O_5$ needles at the extreme free surface, the direct access to the clean surface of interlocked needles responsible also of micro-roughness and the densification of the 3D siloxane network.

Acknowledgements

The authors want to thanks Ivoclar Vivadent for the supply of the lithium disilicate glass-ceramic IPS Emax Press pellets.

REFERENCES

- [1] Shenoy A, Shenoy N. Dental ceramics: an update. *J Conserv Dent* 2010;13(4):195–203, <http://dx.doi.org/10.4103/0972-0707.73379>.
- [2] Matinlinna JP, Lassila LVJ, Ozcan M, Yli-Urpo A, Vallittu PK. An introduction to silanes and their clinical applications in dentistry. *Int J Prosthodont* 2004;17(March–April (2)):155–64.
- [3] Hooshmand T, van Noort R, Keshvan A. Bond durability of the resin-bonded and silane treated ceramic surface. *Dent Mater* 2002;18:179–88.
- [4] Queiroz JR, Benetti P, Ozcan M, de Oliveira LF, Della Bona A, Takahashi FE, et al. Surface characterization of feldspathic ceramic using ATR FT-IR and ellipsometry after various silanization protocols. *Dent Mater* 2012;28:189–96.
- [5] Roulet JF, Söderholm KJ, Longmate J. Effects of treatment and storage conditions on ceramic/composite bond strength. *J Dent Res* 1995;74:381–7.
- [6] Monticelli F, Toledano M, Osorio R, Ferrari M. Effect of temperature on the silane coupling agents when bonding core resin to quartz fiber posts. *Dent Mater* 2006;22:1024–8.
- [7] Shen C, Oh WS, Williams JR. Effect of post-silanization drying on the bond strength of composite to ceramic. *J Prosthet Dent* 2004;91:453–8.
- [8] Fabianelli A, Pollington S, Papacchini F, Goracci C, Cantoro A, Ferrari M, et al. The effect of different surface treatments on bond strength between leucite reinforced feldspathic ceramic and composite resin. *J Dent* 2010;38:39–43.
- [9] Filho AM, Vieira LC, Araújo E, Monteiro Júnior S. Effect of different ceramic surface treatments on resin microtensile bond strength. *J Prosthodont* 2004;13:28–35.
- [10] Bruzi G, Oliveira Carvalho A, Giannini M, Pires Maia H, Magne P. Post-etching cleaning influences the resin shear bond strength to CAD/CAM lithium-disilicate ceramics. *Appl Adhes Sci* 2017;5:17, <http://dx.doi.org/10.1186/s40563-017-0096-6>.
- [11] Della Bona A, Van Noort R. Ceramic surface preparations for resin bonding. *Am J Dent* 1998;11:276–80.
- [12] Magne P, Cascione D. Influence of post-etching cleaning and connecting porcelain on the microtensile bond strength of composite resin to feldspathic porcelain. *J Prosthet Dent* 2006;96:354–61.
- [13] Belli R, Guimarães JC, Filho AM, Vieira LC. Post-etching cleaning and resin/ceramic bonding: microtensile bond strength and EDX analysis. *J Adhes Dent* 2010;12:295–303.
- [14] Peumans M, Van Meerbeek B, Yoshida Y, Lambrechts P, Vanherle G. Porcelain veneers bonded to tooth structure: an ultra-morphological FE-SEM examination of the adhesive interface. *Dent Mater* 1999;15:105–19.
- [15] Jones GE, Boksmann L, McConnell RL. Effect of etching technique on the clinical performance of porcelain veneers. *Quintessence Dent Technol* 1986;10:635–7.
- [16] Bailey LF, Bennett RJ. DICOR® surface treatments for enhanced bonding. *J Dent Res* 1988;67:925–31, <http://dx.doi.org/10.1177/00220345880670060701>.
- [17] Leite FP, Özcan M, Valandro LF, Cunha Moreira CH, Amaral R, Bottino MA, et al. Effect of the etching duration and ultrasonic cleaning on microtensile bond strength between feldspathic ceramic and resin cement. *J Adhes* 2013;89:159–73, <http://dx.doi.org/10.1080/00218464.2013.739024>.
- [18] Steinhäuser HC, Turssi CP, França FMG, Amaral FLBdo, Basting RT. Micro-shear bond strength and surface micromorphology of a feldspathic ceramic treated with different cleaning methods after hydrofluoric acid etching. *J Appl Oral Sci* 2014;22:85–90, <http://dx.doi.org/10.1590/1678-775720130339>.
- [19] Barjaktarova-Valjakova E, Grozdanov A, Guguvcevski L, Korunoska-Stevkovska V, Kapusevska B, Gigovski N, et al. Acid etching as surface treatment method for luting of glass-ceramic restorations, part 1: acids, application protocol and etching effectiveness. *Open Access Maced J Med Sci* 2018;6(3):568–73, <http://dx.doi.org/10.3889/oamjms.2018.147>.
- [20] Ho GW, Matinlinna JP. Insights on ceramics as dental materials. Part II: chemical surface treatments. *Silicon* 2011;3:117–23, <http://dx.doi.org/10.1007/s12633-011-9079-6>.
- [21] Ramakrishnaiah A, Alkheraif AA, Divakar DD, Matinlinna JP, Vallittu PK. The effect of hydrofluoric acid etching duration on the surface micromorphology, roughness, and wettability of dental ceramics. *Int J Mol Sci* 2016;17:822, <http://dx.doi.org/10.3390/ijms17060822>.
- [22] Bischoff C, Eckert H, Appel E, Rheinberger VM, Holand W. Phase evolution in lithium disilicate glass-ceramics based on non-stoichiometric compositions of a multi-component system: structural studies by ^{29}Si single and double resonance solid state NMR. *Phys Chem Chem Phys* 2011;13:4540–51, <http://dx.doi.org/10.1039/c0cp01440k>.
- [23] Puls S, Eckert H. Spatial distribution of lithium ions in glasses studied by 7Li spin echo double resonance. *Phys Chem Chem Phys* 2007;9(30):3992–8, <http://dx.doi.org/10.1039/b705338j>.
- [24] Denry I, Holloway JA. Ceramics for dental applications: a review. *Materials (Basel)* 2010;3:351–68, <http://dx.doi.org/10.3390/ma301035>.
- [25] Upadhyaya GS, Holland W, Beall G. Glass-ceramic technology. Westerville, OH, USA: The American Ceramic Society; 2002. p. 372. ISBN: 1-57498-107-2.
- [26] Kamitsos EI, Yannopoulos YD, Varsamis CP, Jain H. Structure-property correlation in glasses by infrared reflectance spectroscopy. *J Non Cryst Solids* 1997;222:59–68, [http://dx.doi.org/10.1016/S0022-3093\(97\)90097-1](http://dx.doi.org/10.1016/S0022-3093(97)90097-1).
- [27] Shrivastava S, Agrawal S, Parlani S, Saoji S. All ceramic cementation: a key to successful restoration. *Ann Essences Dent* 2014;VI(July–September (3)):35–43, <http://dx.doi.org/10.5368/aedj.2014.6.3.4.5>.
- [28] Chiang C, Koenig JL. Fourier transform infrared spectroscopic study of the adsorption of multiple amino silane coupling agents on glass surfaces. *J Coll Interf Sci* 1981;83:361–70, [http://dx.doi.org/10.1016/0021-9797\(81\)90331-3](http://dx.doi.org/10.1016/0021-9797(81)90331-3).